scientific reports

OPEN

Modeling and control of functional electrical stimulation cycling training system

Mingxu Sun[1,2], Fangyuan Cheng[1], Tingting Wang[1], Chuan Hu[3], Sizhong Wang[4], Xiangyang Li[5], Yuan Xu[1,6] & Min Liu[3]✉

Functional electrical stimulation (FES), a rehabilitation technique, typically relies on physiotherapists using trial-and-error tests to determine effective stimulation patterns. Therefore, this study proposed a kind of pedal hill modeling to establish an optimal stimulus mode with the maximum torque efficiency optimization objective. This study also proposed a new model based on the particle swarm optimization (PSO) algorithm, the back propagation (BP) neural network algorithm, and the proportional integral derivative (PID) control composite algorithm. Six participants were recruited for the experiment. Using the proposed modeling method, we found an appropriate stimulation mode for each of the six subjects, and then each subject performed three sets of experiments for cycling without electrical stimulation, cycling with fixed pulse width, and cycling with adaptive adjustment of pulse width by the fabricated controller. The results of the study showed that root mean square error (RMSE), average (AVE), training time and number of stops all performed well compared to the no control and fixed control conditions and the adaptive pulse width control system of the fabricated controller allows subjects to train at a longer continuous running time and a more stable cycling training speed.

Stroke and spinal cord injury are the two leading causes of damage to the central nervous system, often leading to hemiplegia or paraplegia[1]. Stroke is a clinical manifestation of acute cerebrovascular disease characterized by high morbidity and disability[2]. Hemiplegia can significantly reduce an individual's mobility, usually resulting in altered metabolic function and body composition[3,4]. A damage to the spinal cord can cause either whole or partial paralysis, affecting neuronal signaling and regulation both above and below the site of injury. This can lead to impairments in autonomic, sensory, neuromusculoskeletal, and motor functions[5]. Functional electrical stimulation (FES) is a technique that uses low-frequency electrical pulses to artificially activate paralyzed muscles to produce movements such as walking, grasping and standing[6,7]. FES seeks to assist these individuals in improving or restoring the functional ability of their paralyzed muscles[8]. FES-assisted rehabilitation programs have many benefits, such as pain relief, cardiopulmonary recovery, bone development and metabolic function enhancement[9–11].

FES-assisted cycling is a rehabilitation method that enables people with limb weakness to train on tricycles or stationary cycling trainers[12]. In general, FES-assisted cycling promotes coordinated alternating contractions of specific lower limb muscles in a sequence that varies according to the speed and angle of the ride[13]. There are some FES pedal efficiency issues for traditional FES cycling stimulation mode. Trial-and-error tests are a typical way to find each patient's stimulation pattern during cyclic therapy[14,15]. But the physiotherapist's experience determine show effective the stimulation pattern is. Not only is it a waste of the patient's recovery time, but it also places a burden on the patient and the healthcare provider.

The closed-loop control strategy of FES pedal movement has the potential to provide services with high intensity, low staffing costs and good control accuracy[16–20]. Griffis et al.[21] proposed a closed-loop adaptive based on Deep Neural Networks control scheme for FES cycling to ensure the asymptotic convergence of tracking errors. However, this control method has not been extended to FES control inputs. In previous studies that

[1]School of Electrical Engineering, University of Jinan, Jinan 250022, China. [2]Jinan Key Laboratory of Dyskinesia Rehabilitation and Motor Assessment, Jinan 250021, China. [3]Shandong Provincial Third Hospital, Jinan 250031, China. [4]Department of Health Sciences, Brunel University London, Uxbridge UB8 3PH, UK. [5]Shandong Inspur Intelligent Medical Technology Co., Ltd, Jinan 250101, China. [6]Shandong BetR Medical Technology Co., Ltd, Jinan 250101, China. ✉email: 1770426982@qq.com

adopted adaptive closed-loop control schemes based on proportional-integral-derivative (PID) control algorithms, the fractional-order PID controller proposed by Podlubny demonstrated excellent performance in handling complex dynamic systems[22]. In FES systems, fractional-order controllers have also been attempted to improve control accuracy and system robustness[23]. On the other hand, Wen et al. proposed an observer-based PID controller that exhibited stable performance in controlling random errors and noise influences[24]. For fractional-order controllers, their design and implementation are relatively complex, requiring in-depth mathematical background and significant computational resources, which may be limited in real-time control. Observer-based methods demand high accuracy of the system model; model uncertainties and parameter variations may affect the performance of the observer. However, there are still several problems in the current research phase of using electrical stimulators to help patients with bicycle training. Firstly, Traditional stimulation modes are not able to maintain a steady training speed for long periods of time. Secondly, some studies have used real-time electromyography (EMG) to drive FES system, but the FES generated artifact contaminated EMG signals[25,26]. Thirdly, the PID control algorithm for the adaptive closed-loop control scheme has defects and,has the disadvantages of easy to cause local optimal solutions and slow convergence speed.

Hence, in this study, IMU sensors were used to obtain data to avoid the artifacts generated by FES from polluting the EMG signals, and the stimulation pattern was obtained from the motor rehabilitation of incomplete spinal cord injury patients (T9-T12) using pedaling motion hill modeling and optimizing the target with maximum moment efficiency. We proposed a PSO-BP-PID controller. It has the adaptive ability to adjust control parameters in real-time according to system dynamics, adapting to individual differences among patients. The particle swarm optimization algorithm improves convergence speed, avoiding the problem of traditional PID algorithms easily falling into local optima, enhances computational efficiency, and is easy to deploy and implement in practical systems.

Methods
Establishment of mathematical model
In order to study in depth, the principles of human-system interaction during stirrups movement of patients, a dynamic model of the system was developed. The model consists of a lower limb dynamic model for cycling and a dynamic muscle model.

Lower limb dynamic model for cycling
In the process of FES cycling training, joint torque is generated by muscle contraction to drive the relative movement of each part of the lower extremity. The study demonstrates that electrical stimulation activates muscle fibers, leading to contractions muscle joint angles and angular velocities in knee joint movements. Therefore, joint torque can be directly obtained through the activation of muscle fibers and joint angle. Meanwhile, the transfer of joint torque to crank torque is determined by the position of lower limb movement. To get the right stimulation pattern need to know how the lower limb positions change during the pedaling process. Physically, the pedaling motion can be regarded as a single degree of freedom system, and the kinematic model of pedaling can be established, and then the relative positions of lower limb parts can be obtained through the crank angle.

The following will select the left lower limb movement for analysis. As shown in part (b) of Figure 1, L_t, L_s and L_{cr} represent the thigh, calf and crank length(cm) respectively. The angle between the horizontal line and the thigh, calf, and crank are denoted by θ_1, θ_2 and θ_3, respectively. The hip joint location served as the origin of the coordinate system, while the crank's center was used as (x_c,y_c). Set up a system of equations:

$$\begin{cases} L_t \cos\theta_1 + L_s \cos\theta_2 + L_{cr}\cos\theta_3 = x_c \\ L_t \sin\theta_1 + L_s \sin\theta_2 + L_{cr}\sin\theta_3 = y_c \end{cases} \tag{1}$$

As shown in part (b) of Figure 1, the relationship between θ_3 and θ_{cr} is $\theta_3 = -\theta_{cr}$, substituted in formula (1) to get:

$$\begin{cases} L_t \cos\theta_1 + L_s \cos\theta_2 + L_{cr}\cos\theta_{cr} = x_c \\ L_t \sin\theta_1 + L_s \sin\theta_2 - L_{cr}\sin\theta_{cr} = y_c \end{cases} \tag{2}$$
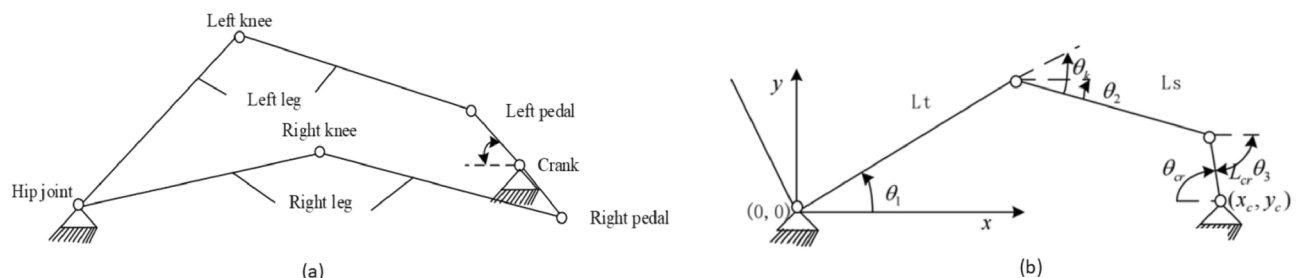

Fig. 1. (**a**) Schematic diagram of FES Cycling training. (**b**) Schematic diagram of unilateral pedal motion structure.

Suppose $a = \frac{L_t}{L_s}$, $b = \frac{y_c + L_{cr}\sin\theta_{cr}}{L_s}$, $c = \frac{x_c - L_{cr}\sin\theta_{cr}}{L_s}$, substituted in formula (2) to get $\begin{cases} \cos\theta_2 = c - a\cos\theta_1 \\ \sin\theta_2 = b - a\sin\theta_1 \end{cases}$. According to the trigonometric formula:

$$l = b^2 - 2ab\sin\theta_1 + a^2\sin^2\theta_1 + c^2 - 2ac\cos\theta_1 + a^2\cos^2\theta_1 \tag{3}$$

$$\theta_1 = \begin{cases} \pi - \arcsin\left(\frac{a^2 + b^2 + c^2 - 1}{2a\sqrt{b^2 + c^2}}\right) - \arctan\frac{c}{b} & \theta_{cr} \in [0, \pi) \\ -\arcsin\left(\frac{a^2 + b^2 + c^2 - 1}{2a\sqrt{b^2 + c^2}}\right) - \arctan\frac{c}{b} & \theta_{cr} \in [\pi, 2\pi) \end{cases} \tag{4}$$

$$\theta_1 - \theta_2 = \arccos\left(\frac{b^2 + c^2 - a^2 - 1}{2a}\right) \tag{5}$$

Through the above calculation, the relation of each bar angle is obtained. Part (b) of figure 1 shows the formula $\theta_h = \theta_1$. According to the above functions, θ_h and θ_k are divided into functions of θ_{cr}, The meanings of θ_h and θ_k are: $\theta_h = f_h(\theta_{cr})$, $\theta_k = f_k(\theta_{cr})$. Taking the time derivative of formula (2), we get the angular velocity W_1 and W_2 of θ_1 and θ_2, $w_1 = -\frac{L_{cr}w\sin(\theta + \theta_1)}{L_t\sin(\theta_1 - \theta_2)}$, $w_2 = -\frac{L_{cr}w\sin(\theta + \theta_2)}{L_t\sin(\theta_2 - \theta_1)}$. where w is the angular velocity of the crank. Taking the second derivative of formula (2) in time, we get the acceleration a_1 and a_1 of θ_1 and θ_2, where a is the acceleration of the crank.

$$a_1 = \frac{\theta_1^2 L_t\cos(\theta_1 + \theta_2) + w_2^2 L_s + aL_{cr}\cos(\theta - \theta_2)}{L_t\sin(\theta_1 - \theta_2)} \tag{6}$$

$$a_2 = \frac{\theta_2^2 L_t\cos(\theta_1 + \theta_2) + w_1^2 L_s + aL_{cr}\cos(\theta - \theta_1)}{L_t\sin(\theta_2 - \theta_1)} \tag{7}$$

The crank torque is calculated by Lagrange method and virtual work principle. First calculate the kinetic energy of the left leg T_l, The kinetic energy of the leg is composed of moving kinetic energy and rotational kinetic energy.

$$T_l = \frac{1}{2}m_t L_t^2\theta_h^2 + \frac{1}{2}I_s\theta_h^2 + \frac{1}{2}m_s\left[L_t^2\theta_h^2 + 2L_t L_s\theta_h\theta_2\cos(\theta_h - \theta_2) + L_s^2\theta_2^2\right] + \frac{1}{2}I_s\theta_2^2 \tag{8}$$

Express T_l relationship with θ_{cr} as a function of $T_l = T(\theta_{cr})\theta_{cr}^2$. The gravitational potential energy is formulated as follows:

$$T_l = L_1\sin\theta_h \times m_t g + (L_1\sin\theta_h + L_2\sin\theta_2) \times m_s g \tag{9}$$

Express V_l relationship with θ_{cr} as a function of $V_l = V(\theta_{cr})$. According to the dynamic analysis of the right leg lags π bar relative to the left leg T_r, can be obtained $T_r = T(\theta_{cr} - \pi)\theta_{cr}^2$, $V_r = V(\theta_{cr})$. The generalized force simplified by the Lagrangian formula is shown below[27] :

$$Q_{cr} = 2[T(\theta_{cr})\theta_{cr} + T(\theta_{cr} - \pi)\theta_{cr}] + \frac{dT(\theta_{cr})}{dt}\theta_{cr} + \frac{dT(\theta_{cr} - \pi)}{dt}\theta_{cr} + \frac{dV(\theta_{cr})}{d\theta_{cr}} + \frac{dV(\theta_{cr} - \pi)}{d\theta_{cr}} \tag{10}$$

Muscle dynamic model
The electrical stimulation causes the muscle contraction process to activate the corresponding muscle fibers, and the degree to which the muscle fibers are activated is the degree of muscle activation. Schematic of the Hill-Huxley model is shown in Figure 2. The formula used to calculate muscle activation is:

$$\text{Act} = \begin{cases} 0, & \text{pw} < \text{Thres} \\ Sf\frac{\text{pw} - \text{Thres}}{\text{Sat} - \text{Thres}}, & \text{Thres} \leq \text{pw} < \text{Sat} \\ Sf, & \text{pw} \geq \text{Sat} \end{cases} \tag{11}$$

Where pw is the pulse width, Thres and Sat are threshold pulse width and saturation pulse width, respectively. The Act is muscle activation in the range of 0–1, sfis scale factor, takes the value of 1. In the second section of the muscle contraction module, muscle force is a function of muscle activation, muscle length, and velocity[28]. To simplify the calculation, the equations for angle and angular velocity are used as relations[29].

$$M_{ma} = \exp\left\{-\left(\frac{\phi - K_1}{K2}\right)^2\right\} \tag{12}$$

$$f_v = 1 + \frac{1}{v_m}\frac{dl}{dt} \tag{13}$$

$$M_{mv} = 1 + \frac{1}{v_m}\frac{dl}{d\phi}\frac{d\phi}{dt} = 1 - \frac{1}{v_m}ma\dot{\phi}(t) = 1 - K_3\dot{\phi} \tag{14}$$
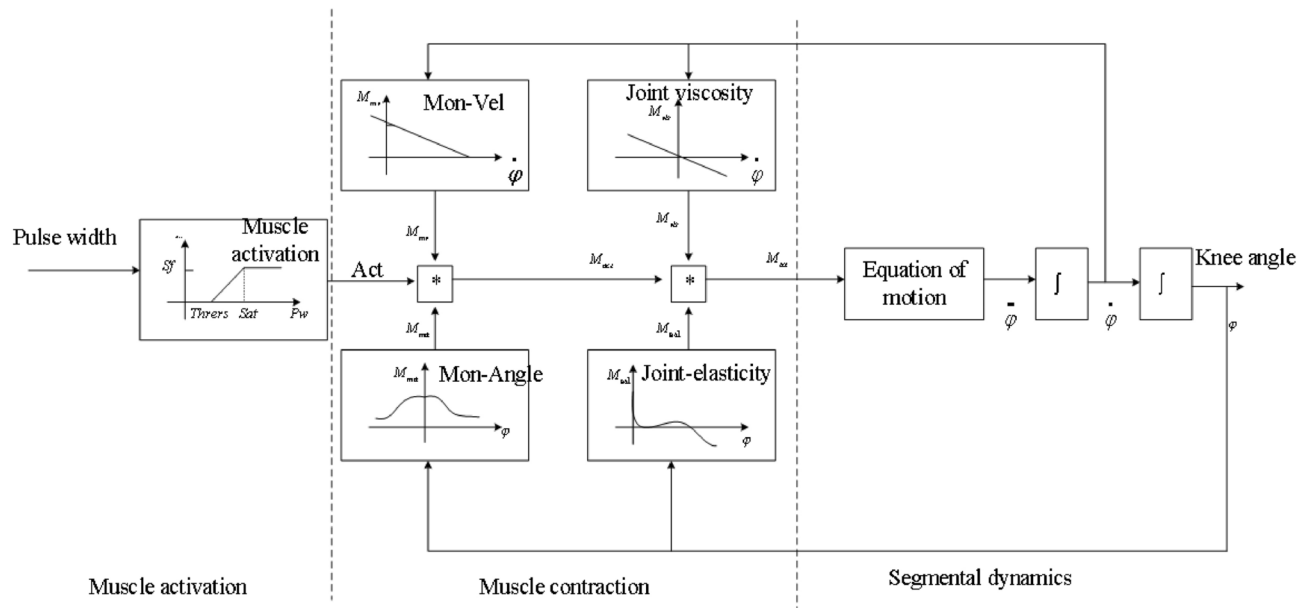
Fig. 2. Schematic of the Hill-Huxley model.

Where ϕ is the knee angle ($0 \leq \phi \leq 180$), M_{ma} is the moment angle coefficient of the knee joint. M_{mv} is the angular velocity coefficient of the moment in the knee joint. l is the length of the quadriceps. V_m is the rate of contraction of the quadriceps. $ma\phi$ is the power of the quadriceps muscle in the knee joint Rule; k_1 and k_2 are two parameters to be identified. Since k_3 is difficult to determine, it is calculated from the available data described in the literature as $k_3 = 0.04$[30,31]. The active torque of muscle activation is $M_{act} = Act \cdot M_{ma} \cdot M_{mv}$. In this model, active and passive muscle attributes are separate. The active moments belong to the active muscle properties. Passive muscle properties were calculated in the third part of muscle contraction dynamics. Passive muscle properties include passive damping moments $M_{vis} = \mu\dot{\phi}$, and passive stiffness moments $M_{cla} = \lambda(\phi - \phi_0)$. Where μ, λ and ϕ_0 represent the hysteresis coefficient, elasticity coefficient and reference angle, respectively. The three parameters μ, λ and ϕ_0 are to be identified. According to the study of Ferrarin[32], The kinetic equation provides the total external moment acting on the knee joint: $J\ddot{\phi} = M_{act} + M_{grav} + M_{vis} + M_{cla}$.

Stimulation pattern
By referring to the existing FES cycling stimulation pattern, it was found that this study used a quantitative method to maximize the torque conversion rate from the knee joint to the crank by using Thres and Sat as the critical constraint values of the controlled object not only coordinates the movement of the leg muscles but also reduces muscle fatigue and maximizes muscle output. The stimulation pattern is related to the equipment model, the subject's training posture and the subject's height and weight information. In this study, the stimulation mode was optimized for the human body work efficiency as the optimization goal.

Firstly, input some basic parameters necessary for the design (human body size, experimental device size, etc.). Secondly, import these parameters into the already built lower limb dynamic model for cycling to obtain the motion state of each part of the lower limb. Thirdly, the effective moment and knee joint moment calculation was performed by combining the motion state with the muscle dynamics model. After the above calculation, it is easy to get the muscle output torque and average muscle energy expenditure during the movement. Finally, enter the calculation of energy efficiency and controller adjusted the intensity of the stimulation to the optimal stimulation mode so that the training in this mode can achieve the maximum average efficiency.

Calculation formula of instantaneous working efficiency in FES cycling: $\eta = \frac{1}{Angle} \int_{A_1}^{A_2} \frac{Q_{cr}}{M_{act}}$. Where Q_{cr} is torque at the crank, M_{act} is torque at the knee joint, Angle is the angular interval, A_1 and A_2 is the initial angle and the termination angle of the stimulus, respectively. The stimulation angle interval was selected after the references as 100[16,33,34].

Controller design
In order to achieve stable cycling in FES cycling, the PID controller was used to adjust the stimulus signal PW. The particle swarm optimization approach was proposed to optimize the BP neural network's connection weight matrix in order to accelerate the learning convergence speed and keep it from entering local minima.
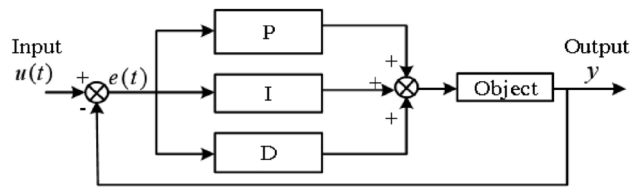
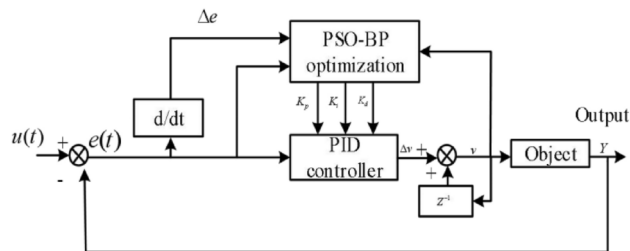**Fig. 3.** Basic structure of PID control system.

Fig. 4. Basic structure of PSO-BP-PID control system.

PID controller

Figure 3 depicts the PID control system's fundamental architecture. The PID controller consists of three links: proportional, integral and differential, which are described mathematically as follows:

Where K_p is a scale factor, T_i is integration time constant, and T_d is differential time constant. The proportional link instantly reflects the deviation signal $e(t)$ proportionally, and the controller immediately generates a control effect to reduce it through negative feedback. The integral link is used to eliminate the static difference to improve the non-differential degree of the system. In contrast, the system's performance indices acquired by the conventional tuning procedure are frequently subpar when dealing with complicated real-world controlled objects, such significant overshoot and lengthy correction times. The popular BP neural network offers high self-adaptability and self-learning capabilities for complicated and unpredictable applications. It has infinite accuracy for approximating any continuous nonlinear function.

PSO-BP-PID controller

The basic structure of the PSO-BP-PID control system is shown in Figure 4, where u(t) is the expected riding speed given by the system; v is the pulse width of the electrical stimulator in the system; Y is the actual speed at which the system expects the cycling training; e(t) is the error between the actual velocity and the expected velocity.

The basic idea behind PSO is to start with a collection of particles that have no mass or volume. Then, each particle is viewed as a potential solution to the particular kind of optimization issue, and the set fitness function is used to assess the particle quality[35]. The particle swarm optimization algorithm can be mathematically described as follows[36]:

$$v_{id}^{t+1} = wv_{id}^{t} + c1^*rand()^*(p_{id} - x_{id}^{t}) + c2^*rand()^*(p_{gd} - x_{id}^{t}) \tag{15}$$

$$x_{id}^{t+1} = x_{id}^{t} + v_{id}^{t+1} \tag{16}$$

Where r_1 and r_2 are random numbers between 0 and 1; c_1 and c_2 are acceleration constants, which represent the degree to which particles are influenced by social knowledge and individual cognition and are usually set to the same value. The w is the inertia weight factor, which is used to balance the global exploration and local development ability of particles. v_{id}^{t} and x_{id}^{t} are the velocity and position of the d dimension of particle i in the t iteration, respectively. p_{id} is the individual extreme position of particle i in the d dimension and p_{gd} is the global extreme position of the population in the d dimension. The BP neural network is widely used as a feedback network[37,38]. The basic idea of the BP-PID algorithm is to make the three neurons of output layer correspond to the three parameters of proportion, integral and differential in the PID structure. With the help of the self-learning capacity for the neural network, the output of the PID coefficient is controlled by adjusting the weight coefficient between layers. The structure of the BP neural network is shown in Figure 5.

Experimental

Apparatus and system

To prevent subjects from having excessive lower limb movements, we designed an ankle-foot orthosis and fixed subjects' lower limbs to the pedals. Using a modified pedal bike as an experimental platform, each lower leg was
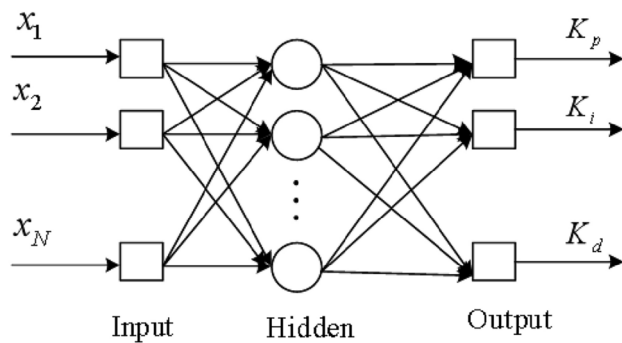
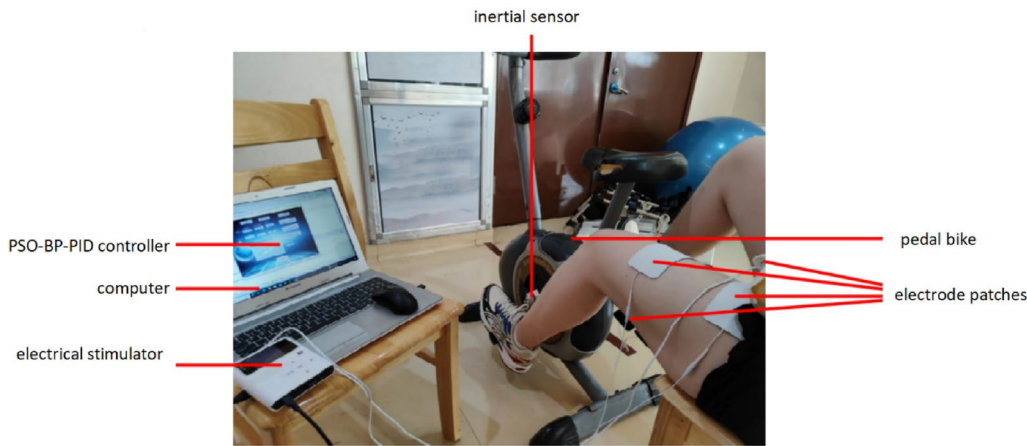**Fig. 5**. The structure of the BP neural network.

Fig. 6. Schematic diagram of the experimental scene.

Sex (male/female)	1/6
Age range (years)	22–58
Etiology (healthy/spinal cord injury/stroke)	1/3/3
Spinal cord injury score range	T9-T12
Stroke score range	1–6

Table 1. Characteristics of subjects (N=7).

inserted into a fixation device fixed to the pedal so that leg movement was restricted to the sagittal plane. An inertial sensor was used to obtain the crank angle, and the stimulation pattern was implemented according to the crank angle. A personal computer was used to collect the crank angle data through a frequency of 200 Hz, and the individual controlled the electrical stimulator through a USB interface via the computer USB interface. Pulse width modulation (threshold-saturation) was used with balanced bipolar stimulation pulses with a constant frequency (20 Hz) and amplitude. The pedaling rhythm was maintained at a constant rate by the intensity of the stimulation delivered to the muscle. Schematic diagram of the experimental scene is shown in Figure 6.

Subjects
We recruited six subjects from July to September 2022 at Shandong Provincial Third Hospital. The study has been approved by the Medical Ethics Committee of Shandong Provincial Third Hospital (KYLL-2020023). All subjects signed the informed consent form. All methods were performed in accordance with the relevant guidelines and regulations. The characteristics of the subjects are shown in Table 1. All subjects had no severe cognitive or communication problems. From Table 1, we can see that the study covered patients with different lower limb movement disorders. Subject 1 was a healthy person; subject 2, subject 4, and subject 6 were spinal cord injury patients; subject 3, and subject 5 were stroke patients. We selected stroke patients who had The NIH stroke scale (NIHSS) scores of 1–6. The NIHSS scoring system are: 0 = no stroke;1–4 = minor stroke; 5–15 = moderate stroke; 15–20 = moderate/severe stroke; 21–42= severe stroke[17]. The Hospital Ethics Committee approved the study, and all subjects signed informed consent. All subjects had no severe cognitive or communication problems.

We collected all subjects' characteristics, including information on height, weight, electrical stimulation pulse width threshold and saturation value. Each subject underwent three trials: (1) experiment without an electrical stimulator (traditional training), (2) experiment with a fixed electrical stimulation pulse width (training with fixed pulse width), and (3) experiment with the designed controller controlling the stimulation pulse width (training with self-adaptation control). Each experiment lasted 30 min with an interval of one day between tests to avoid muscle fatigue. And the experiments were executed sequentially, at a fixed point in time each day.

Performance indexes
An indicator of tracking accuracy is the root mean square error(RMSE).

$$\text{RMSE} = \sqrt{\frac{1}{T} \sum_{t=1}^{T} (x(t) - x_d(t))^2} \tag{17}$$

Where x denotes cycling speed, x_{dis} the desired speed, and T is the duration of cycling training. The absolute value of error (AVE)fluctuations was calculated as a measure of velocity fluctuations.The formula for AV is: $\text{AVE} = \max(x_n) - \min(x_n)$ Where $\max(\cdot)$ is to take the maximum value, $\min(\cdot)$ is to take the minimum value. The training duration and number of stops were calculated as a facilitation of FES.

Results

Figure 7 shows the results of a thirty-minute cycling experiment with two subjects are shown: Traditionally trained cycling speed, training with fixed pulse width cycling speed and training with self-adaptation control cycling speed. In the experiment, it was found that the change in pulse width in a short period of time had little effect on the running speed, so the average running speed of three revolutions was used as the running speed of the FES rehabilitation vehicle. We can see from Figure 7 that the subjects using the adaptive control scheme had a more stable cycling speed.

From Table 2, it is evident that under the conditions of electrical stimulation, the mean squared deviations are rather minimal. Table 3 shows that under the condition of FES participation, the speed mean square deviation of cycling training is relatively small, and in the three conditions using adaptive control were reduced in order. For example, Subject 6 had a self-adaptation control reduction of 0.644 and 0.7402 units compared to the traditional training mode and the fixed electrical stimulation mode, respectively. However, for subject 1, the velocity fluctuations in the conventional condition were smaller. Subjects' actual cycling time (minus the intervening pauses for rest) during the thirty-minute subject time can be obtained from Table 4. It can be seen that the effective cycling time in the fixed pulse width electrical stimulation condition was greater than the conventional cycling time. The effective cycling time in the adaptive control electrical stimulation condition was greater than the cycling time in the fixed pulse width electrical stimulation condition. For example, the Cycling time of subject 2 in training with self-adaptation control was 578 s and 152 s longer than that of the traditional training
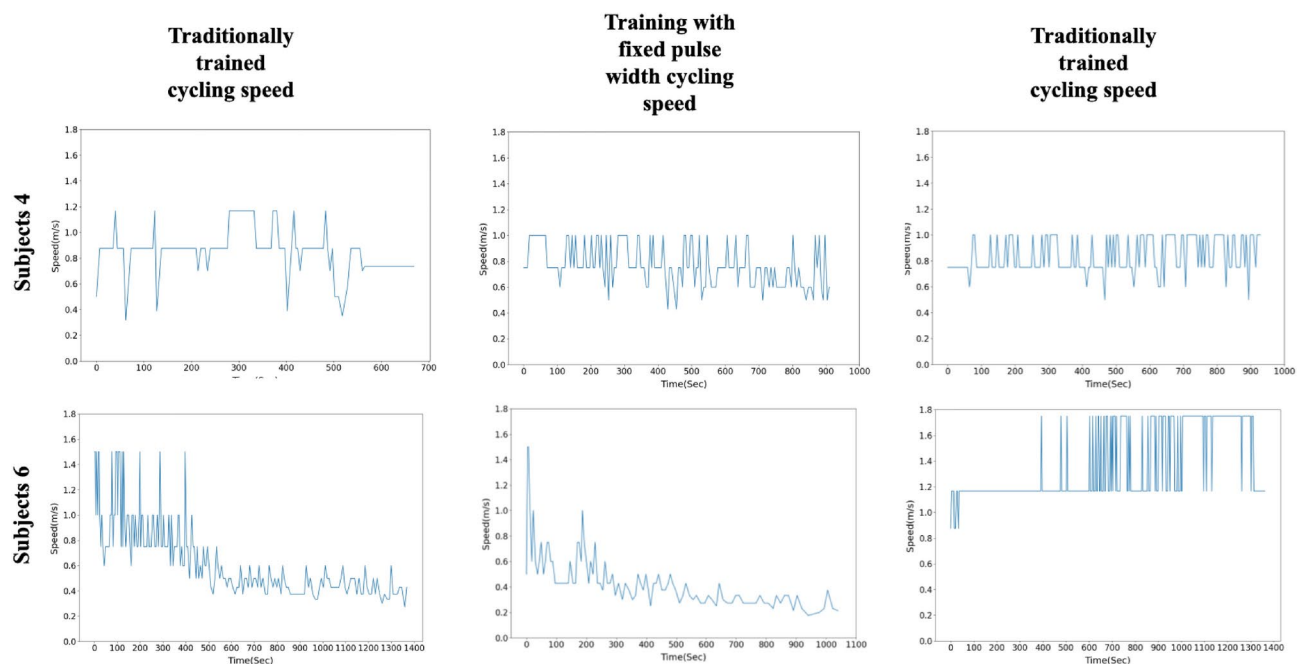

Fig. 7. Different training modes cycling speed for subject 4 and subject 6.

Train mode	Subjects					
	Subject1	Subject2	Subject3	Subject4	Subject5	Subject6
RMSE of subjects speed in training with fixed pulse width(m/s)	0.0027	0.0008	0.0013	0.0025	0.0023	0.0027
RMSE of subjects speed in training with self-adaptation control(m/s)	0.0017	0.0008	0.0017	0.0024	0.0032	0.0053

Table 2. RMSE of subjects speed in different training modes.

Train mode	Subjects					
	Subject1	Subject2	Subject3	Subject4	Subject5	Subject6
Traditional training	0.3111	0.6250	0.7778	0.8485	1.3611	1.2273
Training with fixed pulse width	0.7500	0.3750	0.5357	0.5714	1.2273	1.3235
Training with self-adaptation control	0.6250	0.3750	0.5000	0.5000	0.5714	0.5833

Table 3. The Ave of subjects speed in different training modes.

Train mode	Subjects					
	Subject1	Subject2	Subject3	Subject4	Subject5	Subject6
Cycling time of subjects in traditional training(s)	941	534	1411	669	1175	1361
Cycling time of subjects in training with fixed pulse width(s)	1115	960	1443	910	1510	1039
Cycling time of subjects in training with self-adaptation control(s)	1028	1112	1439	929	820	1368
The number of cycling pauses in traditional training	3	1	1	1	1	0
The number of cycling pauses in training with fixed pulse width	1	1	0	0	0	0
The number of cycling pauses in training self-adaptation control	1	1	0	0	0	0

Table 4. Cycling time of subjects and the number of cycling pauses in different training modes.

mode and the fixed electrical stimulation mode, respectively. However, for subject 5, the cycling experiment in the adaptive control condition ended early without waiting for the end of the training condition, so there is a short ride time in the adaptive controller mode.

The experimental results show that the FES control system is more stable than both the traditional cycling mode and the fixed pulse width mode. Specifically,

$$\text{RMSE}_{\text{Fixed Pulse Width}} < \text{RMSE}_{\text{Self-adaptation Control}}$$
$$\text{AVE}_{\text{Self-adaptation Control}} < \text{AVE}_{\text{Fixed Pulse Width}} < \text{AVE}_{\text{Tranditional Traing Mode}}$$
$$\text{Training Time}_{\text{Traditional Training Mode}} < \text{Training Time}_{\text{Fixed Pulse Width}} < \text{Training Time}_{\text{Self-adaptation Control}}$$
$$\text{Number of Stops}_{\text{Self-adaptation Control}} < \text{Number of Stops}_{\text{Fixed Pulse Width}} < \text{Number of Stops}_{\text{Traditional Training Mode}}$$

Therefore, the FES rehabilitation vehicle control system proposed in this study has good control performance for rehabilitation cycling training.

Discussion

The experimental results clearly show that by studying patients with different levels of severity, we have found that the worse the lower limb movement is for a given patient type, the better the control of the FES adaptive controller is. The traditional FES cycling stimulation pattern is still based on the experience of physiotherapist and is a fixed pattern[16,39]. This not only makes the rehabilitation of patients less efficient but also requires a large number of experienced physiotherapists. Our research is more stable than the optimization of other control algorithms, The RMSE achieved in our study was 4 units lower than that reported by NBoudville et al. (2018)[40], 1.1 units lower than the results of Rouhani et al. (2017)[41], and 0.16 units lower than the findings of de Sousa et al. (2016)[42].

One of the main contributions of our research work is the proposed automatic stimulation timing based on the patient's characteristics. The stimulation pattern can be obtained after the first measurement of the patient's body parameters and can be used later in the training process. The stimulation pattern can be obtained dynamically from each patient to suit his or her needs. Another major contribution of this study is the proposed

method of adaptive control of the FES. In this study, We proved this method can easily deploy on other systems and not require manual adjustment of the stimulation intensity and allows adaptive adjustment of the assisted stimulation pulse width according to the rehabilitation training speed of each patient. But we also faced the common limitation about may not reflect the true effect in larger or more heterogeneous populations due to the small sample size, resulting in limited external validity. The proposed modeling method requires more parameters to be identified, and therefore more preparatory experiments are needed.

There are some limitations in this study. We only recruited few participants. Future research should strengthen collaboration with healthcare organizations to access larger and more diverse datasets, enhancing the external validity of the findings and addressing potential underlying. Additionally, in terms of application, the developed model should be further optimized to achieve lightweight implementation without compromising accuracy, making it more feasible for deployment on endpoint devices.

Conclusion

In this study, pedal hill modeling was used to find the optimal stimulus mode with the maximum torque efficiency optimization objective, and the PSO-BP-PID control algorithm was used to construct the adaptive controller system. We found that the designed adaptive controller can effectively make the subjects cycling steadily at the expected speed. These results provide the possibility that subjects have longer continuous training times and more stable circuit training speeds during training.

Data availability

The datasets generated and/or analyzed during the study are limited due to data confidentiality reasons, which are used under the license of this study and are therefore not publicly available. However, if they makes a reasonable request and obtains permission from the Shandong Provincial Third Hospital, the corresponding author can be contacted to obtain the data.

References

1. Abdullayeva, G. M., Batyrhanov, S. K., Akhunbaev, S. M. & Uzakov, O. J. The effects of nutritional support for premature babies with elbw and vlbw with hypoxic damage to the central nervous system. *Heart, Vessels and Transplantation* **4**, 45–54 (2020).
2. Li, F. et al. Stock market fluctuation and stroke incidence: A time series study in eastern china. *Social Science & Medicine* **296**, 114757 (2022).
3. Gorgey, A. S., Poarch, H. J., Dolbow, D. R., Castillo, T. & Gater, D. R. Effect of adjusting pulse durations of functional electrical stimulation cycling on energy expenditure and fatigue after spinal cord injury. *Journal of Rehabilitation Research & Development* **51** (2014).
4. Silva, N. A., Sousa, N., Reis, R. L. & Salgado, A. J. From basics to clinical: a comprehensive review on spinal cord injury. *Progress in neurobiology* **114**, 25–57 (2014).
5. Varma, A. K. et al. Spinal cord injury: a review of current therapy, future treatments, and basic science frontiers. *Neurochemical research* **38**, 895–905 (2013).
6. Barss, T. S. et al. Utilizing physiological principles of motor unit recruitment to reduce fatigability of electrically-evoked contractions: a narrative review. *Archives of physical medicine and rehabilitation* **99**, 779–791 (2018).
7. Takeda, K., Tanino, G. & Miyasaka, H. Review of devices used in neuromuscular electrical stimulation for stroke rehabilitation. *Medical Devices: Evidence and Research* 207–213 (2017).
8. Gibbons, R. S., Beaupre, G. S. & Kazakia, G. J. Fes-rowing attenuates bone loss following spinal cord injury as assessed by hr-pqct. *Spinal Cord Series and Cases* **2**, 1–4 (2016).
9. Sarabadani Tafreshi, A., Okle, J., Klamroth-Marganska, V. & Riener, R. Modeling the effect of tilting, passive leg exercise, and functional electrical stimulation on the human cardiovascular system. *Medical & biological engineering & computing* **55**, 1693–1708 (2017).
10. Gorgey, A. S., Dolbow, D. R., Dolbow, J. D., Khalil, R. K. & Gater, D. R. The effects of electrical stimulation on body composition and metabolic profile after spinal cord injury-part ii. *The journal of spinal cord medicine* **38**, 23–37 (2015).
11. Gorgey, A. S., Graham, Z. A., Bauman, W. A., Cardozo, C. & Gater, D. R. Abundance in proteins expressed after functional electrical stimulation cycling or arm cycling ergometry training in persons with chronic spinal cord injury. *The journal of spinal cord medicine* **40**, 439–448 (2017).
12. Bo, A. P. et al. Cycling with spinal cord injury: a novel system for cycling using electrical stimulation for individuals with paraplegia, and preparation for cybathlon 2016. *IEEE Robotics & Automation Magazine* **24**, 58–65 (2017).
13. Fattal, C. et al. Training with fes-assisted cycling in a subject with spinal cord injury: Psychological, physical and physiological considerations. *The Journal of Spinal Cord Medicine* **43**, 402–413 (2020).
14. Gfohler, M. & Lugner, P. Cycling by means of functional electrical stimulation. *IEEE Transactions on Rehabilitation Engineering* **8**, 233–243 (2000).
15. Perkins, T. A., Donaldson, N. N., Hatcher, N. A., Swain, I. D. & Wood, D. E. Control of leg-powered paraplegic cycling using stimulation of the lumbo-sacral anterior spinal nerve roots. *IEEE Transactions on Neural systems and rehabilitation engineering* **10**, 158–164 (2002).
16. Chen, J., Yu, N.-Y., Huang, D.-G., Ann, B.-T. & Chang, G.-C. Applying fuzzy logic to control cycling movement induced by functional electrical stimulation. *IEEE transactions on rehabilitation engineering* **5**, 158–169 (1997).
17. Hunt, K. J. et al. Control strategies for integration of electric motor assist and functional electrical stimulation in paraplegic cycling: utility for exercise testing and mobile cycling. *IEEE Transactions on Neural systems and rehabilitation engineering* **12**, 89–101 (2004).
18. Kim, C.-S. et al. Stimulation pattern-free control of fes cycling: Simulation study. *IEEE Transactions on Systems, Man, and Cybernetics, Part C (Applications and Reviews)* **38**, 125–134 (2007).
19. Liu, Q. et al. A fully connected deep learning approach to upper limb gesture recognition in a secure fes rehabilitation environment. *International Journal of Intelligent Systems* **36**, 2387–2411 (2021).
20. Zouari, F., Ibeas, A., Boulkroune, A. & Cao, J. Finite-time adaptive event-triggered output feedback intelligent control for noninteger order nonstrict feedback systems with asymmetric time-varying pseudo-state constraints and nonsmooth input nonlinearities. *Communications in Nonlinear Science and Numerical Simulation* **136**, 108036 (2024).

21. Griffis, E. J., Isaly, A., Le, D. M. & Dixon, W. E. Deep neural network-based adaptive fes-cycling control: A hybrid systems approach. In *2022 IEEE 61st Conference on Decision and Control (CDC)*, 3262–3267, (2022). https://doi.org/10.1109/CDC51059.2022.9993025.

22. Podlubny, I. Fractional-order systems and pi/sup /spl lambda//d/sup /spl mu//-controllers. *IEEE Transactions on Automatic Control* **44**, 208–214. https://doi.org/10.1109/9.739144 (1999).

23. Tepljakov, A. et al. Towards industrialization of fopid controllers: A survey on milestones of fractional-order control and pathways for future developments. *IEEE Access* **9**, 21016–21042. https://doi.org/10.1109/ACCESS.2021.3055117 (2021).

24. Wen, P., Dong, H., Huo, F., Li, J. & Lu, X. Observer-based pid control for actuator-saturated systems under binary encoding scheme. *Neurocomputing* **499**, 54–62. https://doi.org/10.1016/j.neucom.2022.05.035 (2022).

25. Chen, J.-J. & Yu, N.-Y. The validity of stimulus-evoked emg for studying muscle fatigue characteristics of paraplegic subjects during dynamic cycling movement. *IEEE transactions on rehabilitation engineering* **5**, 170–178 (1997).

26. Islam, M. A. et al. Mechanomyography responses characterize altered muscle function during electrical stimulation-evoked cycling in individuals with spinal cord injury. *Clinical Biomechanics* **58**, 21–27. https://doi.org/10.1016/j.clinbiomech.2018.06.020 (2018).

27. Z.d.Sun. *Research on knee motion control method based on functional electrical stimulation*. Master's thesis, Suzhou university (2020).

28. Kristianslund, E., Krosshaug, T. & Van den Bogert, A. J. Effect of low pass filtering on joint moments from inverse dynamics: implications for injury prevention. *Journal of biomechanics* **45**, 666–671 (2012).

29. Zajac, F. E. Muscle and tendon: properties, models, scaling, and application to biomechanics and motor control. *Critical reviews in biomedical engineering* **17**, 359–411 (1989).

30. Riener, R. & Fuhr, T. Patient-driven control of fes-supported standing up: a simulation study. *IEEE Transactions on rehabilitation engineering* **6**, 113–124 (1998).

31. Quintern, J., Riener, R., Volz, S., Rupprecht, S. & Straube, A. *Inverse model for control movement* (Springer-Verlag, Berlin, Germany, 1996).

32. Riener, R., Ferrarin, M., Pavan, E. E. & Frigo, C. A. Patient-driven control of fes-supported standing up and sitting down: experimental results. *IEEE Transactions on rehabilitation engineering* **8**, 523–529 (2000).

33. Ferrarin, M., D'acquisto, E., Mingrino, A. & Pedotti, A. An experimental pid controller for knee movement restoration with closed loop fes system. *In Proceedings of 18th Annual International Conference of the IEEE Engineering in Medicine and Biology Society* **1**, 453–454 (1996) (**IEEE**).

34. Eser, P. C., Donaldson, N. N., Knecht, H. & Stussi, E. Influence of different stimulation frequencies on power output and fatigue during fes-cycling in recently injured sci people. *IEEE Transactions on neural systems and rehabilitation engineering* **11**, 236–240 (2003).

35. Simpkins, A. System identification: Theory for the user, (ljung, l.; 1999)[on the shelf]. *IEEE Robotics & Automation Magazine* **19**, 95–96 (2012).

36. Yang, J. et al. Study and design on suspended permanent maglev rail transit system. *Journal of the China Railway Society* **42**, 30–37 (2020).

37. Kennedy, J. & Eberhart, R. Particle swarm optimization. *In Proceedings of ICNN'95-international conference on neural networks* **4**, 1942–1948 (1995) (**ieee**).

38. Wu, H., Liu, Q. & Liu, X. A review on deep learning approaches to image classification and object segmentation. *Computers, Materials & Continua* **60** (2019).

39. Nih-stroke-scale. https://www.ninds.nih.gov/health-information/public-education/know-stroke/health-professionals/nih-stroke-scale. Accessed on July 9, 2024.

40. Boudville, R. *et al.* Development and optimization of pid control for fes knee exercise in hemiplegic rehabilitation. In *2018 12th International Conference on Sensing Technology (ICST)*, 143–148, (2018). https://doi.org/10.1109/ICSensT.2018.8603628.

41. Rouhani, H., Same, M., Masani, K., Li, Y. Q. & Popovic, M. R. Pid controller design for fes applied to ankle muscles in neuroprosthesis for standing balance. *Frontiers in Neuroscience* **11**, (2017). https://doi.org/10.3389/fnins.2017.00347.

42. de Sousa, A. C. C., Ramos, F. M., Dorado, M. C. N., da Fonseca, L. O. & Bó, A. P. L. A comparative study on control strategies for fes cycling using a detailed musculoskeletal model. *IFAC-PapersOnLine* **49**, 204–209 (2016).

Author contributions
Conceptualization, M.S., F.C., C.H. and M.L.; methodology, M.S., F.C. and Y.X.; software, M.S. and F.C.; validation, M.S., F.C., T.W. and C.H.; validation, M.S., F.C. and S.W.; formal analysis, M.S. and F.C.; investigation, M.L. and F.C.; resources, M.S., F.C. and M.L.; writing-original draft preparation, M.S., F.C. and M.L.; writing-review and editing, M.S., F.C. and S.W.; visualization, M.S., F.C. and Y.X.; All authors have read and agreed to the published version of the manuscript.

Declarations

Competing interests
The authors declare that the research was conducted in the absence of any commercial or financial relationships that could be construed as a potential conflict of interest. The corresponding author is responsible for submitting a competing interests statement on behalf of all authors of the paper.

Informed consent statement
Informed consent was obtained from all subjects involved in the study. Written informed consent has been obtained from the patients to publish this paper.

Additional information
Correspondence and requests for materials should be addressed to M.L.